ELSEVIER

Biophysical Chemistry 95 (2002) 211–225

Biophysical Chemistry

www.elsevier.com/locate/bpc

Roles of hydration water molecules in molecular packing of the killer toxin from *Pichia farinosa* in its crystalline state investigated by cryogenic X-ray crystallography

Masayoshi Nakasako[a,*], Fumihiko Tsuchiya[b], Yoji Arata[b]

[a]*Precursory Research for Embryonic Science and Technology (PRESTO), Japan Science and Technology Corporation (JST) and Institute of Molecular and Cellular Biosciences, The University of Tokyo, Yayoi, Bunkyo-ku, Tokyo 113-0032, Japan*

[b]*Water Research Institute, Sengen 2-1-6, Tsukuba, Ibaraki 305-0047, Japan*

Received 25 March 2001; accepted 19 July 2001

Abstract

The hydration structures around the killer toxin from *Pichia farinosa* were investigated by cryogenic X-ray crystallography. In particular, those contributing to the molecular association and the crystal contacts were analyzed with respect to the geometry and the networks of hydrogen bonds. The hydration water molecules attached on the surface so as to make up the surface shape in the contact complementary and mediated the intermolecular interactions through the networks of hydrogen bonds. Careful inspection of the contact area led to a proposal as to the molecular association mode of the toxin to determine the biological function in cells. In addition, the water-associated protein–protein interactions were approximated well by a simple theoretical equation on the solvation force expected in confined geometry. The present analysis may provide a way to analyze the crystal contact and molecular recognition in macromolecules in aqueous solution.

Keywords: Killer toxin; Cryogenic X-ray crystal structure analysis; Hydration structure; Crystal contact; Solvent in the confined geometry

1. Introduction

In crystallization of proteins, spontaneous and ordered nucleation of protein molecules occurs in the presence of precipitant reagents, within specific temperature ranges and under the pH conditions near the iso-electric points of protein molecules [1,2]. The ordered aggregation of proteins is stabilized by various, often weak, types of intermolecular interactions: monopole–monopole, monopole–dipole, dipole–dipole, van der Waals hydrophobic contacts and hydrogen bonds [3]. In a very rough approximation, the intermolecular attractive interactions are described by the Derjaguin–Landau–Verwey–Overbeek theory in the theoretical point of view [3,4]. However, the

*Corresponding author. Present address: Department of Physics, Faculty of Science and Engineering, Keio University, 3-14-1 Hiyoshi, Kohoku-ku, Yokohama 223-8522, Japan.

E-mail address: nakasako@iam.u-tokyo.ac.jp (M. Nakasako).

0301-4622/02/$ - see front matter
PII: S0301-4622(01)00258-7

detailed interactions inducing the crystalline aggregate of protein molecules should be analyzed based on the atomic models of proteins. The analysis may provide clues for discussing the intermolecular interactions of macromolecules in cells, such as protein–protein, antigen–antibody [5,6], protein–DAN [7,8] and receptor–protein complexes [9].

The crystal structure analyses of proteins have provided much structural information as to the inter-molecular interaction modes of proteins in the crystal contact area [10]. The interaction modes are classified into the three types: (i) direct protein–protein interactions; (ii) indirect interactions mediated by ions or small molecules existing in the crystallization buffers; and (iii) indirect ones mediated by hydration water molecules. While the first two modes have been analyzed well, the last one has remained to be elucidated. Because mobile hydration water molecules are inappreciable in the scattering density maps obtained at ambient temperatures, it is difficult to approach the hydration structures contributing to crystal contacts in the detail.

In recent years, cryogenic X-ray diffraction method has been applied to reduce X-radiation damage of protein crystal [11]. At cryogenic temperatures, hydration structures around proteins appear far clearer than at ambient temperatures, because hydration water molecules bind strongly and reside persistently in hydration sites at cryogenic temperatures. Some cryogenic crystal structure analyses have provided new insights into the hydration structures of proteins as to the amount, the interaction geometry and the networks of hydrogen bonds induced in hydration shells [12–15]. In the physico-chemical point of view, the analyses may give a fruitful structural database for discussing the intermolecular surface forces and the behavior of water molecules in confined geometry [16].

In the present study, we selected the killer toxin from halotorelant yeast, *Pichia farinosa*, [17] in its crystalline state as a research target. The toxin molecule secreted from the yeast is composed of two distinct polypeptide chains α (63 amino acid residues) and β (77 residues) (αβ hetero-dimer). The molecule works as a 'killing' factor for bacteria, which is sensitive to the toxin. Various strategies for explaining the killer activity of the toxin has been proposed and examined. The functional unit of the toxin is the hetero-dimer in solution [19], and the toxin exhibits maximum killer activity under acidic pH conditions in vitro. However, the dimer irreversibly dissociates into the two polypeptide chains under the physiological pH conditions above pH 6 in vitro [20,21]. Therefore, any association mode of toxin molecules preventing the dissociation is expected to realize the killer effect under the physiological condition of neutral pH [22].

In a crystalline state, $\alpha_2\beta_2$ hetero-tetramer occupies a crystallographic asymmetric unit [22] and has three types of intermolecular interaction modes for the ordered molecular packing. Because the crystals appearing in the presence of ammonium sulfate or polyethylene glycol 4000 near pH 3.5 [18] are crystallographically identical, hydration mediated intermolecular interaction modes may have significant contribution to the ordered nucleation and the association of toxin molecules. Thus, in the present cryogenic structure analysis, we analyzed the hydration-mediated intermolecular interactions in the crystal. Based on the results, we discuss the possibility that any molecular association mode in the crystalline state may be realized for the toxic function in the physiological pH condition. In addition, the distribution of hydration water molecules engaged in the crystal contacts is compared with the physico-chemical theory on solvent molecules in confined geometry [23,24].

2. Materials and methods

2.1. Crystal structure determination

The killer toxin was prepared and crystallized according to the procedure reported previously [17,18]. In this study, ammonium sulfate was used as a precipitant at a concentration of 2.7 M, and the pH of the crystallization mother liquor was set at 3.5.

X-Ray diffraction intensity data were collected at 112 K by means of the oscillation method with a Raxis-IV system (Rigaku, Japan), an Ultrax18 X-ray generator (Rigaku, Japan) and a double-

mirror focusing optics (Rigaku, Japan). The X-ray generator was operated at a load of 4.05 kW (45 kV, 90 mA), and the CuKα radiation was selected with a nickel foil of 3.8 μm thickness. During the cryogenic experiments, crystals were continuously cooled using the cold nitrogen gas produced from a cooling device (Rigaku, Japan). The camera distance was set at 120 mm.

Before flash-cooling [11], crystals were embedded in a mineral oil, and the crystallization mother liquor surrounding the crystals was carefully removed using a crystal-mounting device (Hampton Research, USA). Then, crystals were picked up with the device and cooled with liquid-ethane. The cooled crystals were transferred to the goniometer of the Raxis-IV system under a cold nitrogen atmosphere below 110 K. The collected diffraction data were indexed, integrated and processed with the program DENZO/SCALEPACK [25] (Table 1).

The starting model for the crystal structure refinement was made by removing solvent molecules from the model determined at ambient temperature [22] [the accession code in the Protein Data Bank (PDB) [26] is 1 KVD [22]]. The crystallographic structure refinement and the model building were carried out with the programs X-PLOR [27] and turboFRODO (Biographics, France), respectively. Rounds of the ordinary refinement protocol were carried out under a set of restraint parameters [28]. Hydration water molecules were picked up from the $[F_o - F_c]$ difference Fourier maps, using the program FESTKOP [12,15], in taking the geometry of hydrogen bonds into account. Newly introduced solvent molecules were examined with omit-annealed $[F_o - F_c]$ difference Fourier maps throughout the subsequent refinement rounds. The statistics of the refined model are summarized in Table 1.

2.2. Hydration structure analysis

The program FESTKOP [12,15] was applied to analyze the hydration structures of proteins as to the geometry and the networks of hydrogen bonds induced in hydration shells. In the first stage of the analysis, hydration water molecules were classified into four groups, 'inside', 'contact', 'first-layer' and 'second-layer', according to their locations relative to the solvent accessible surface (SAS) [29] of the toxin molecule (Table 1). The water molecules belonging to the 'inside' class were located inside the SAS. The molecules in the 'contact' class mediated the interaction between protein molecules related by crystallographic symmetries. The molecules in the 'first-layer' class were located outside the SAS and interacted directly with protein atoms via hydrogen bonds and/or van der Waals interactions. The rest having no direct interactions with protein atoms are termed as 'second-layer'. In the present analysis, the upper limits for distances in hydrogen bonds and van der Waals contacts were set at 3.4 and 3.7 Å, respectively.

3. Results

Crystal structure of the killer toxin was refined at a resolution of 2.1 Å (Fig. 1) enough for separating the individual hydration water molecules in electron density maps (Fig. 2). The crystal structure at 112 K was almost the same with that at ambient temperature [22] as indicated by r.m.s. difference value of main chain atoms less than 0.5 Å and the linear expansion coefficient [30] of less than 5×10^{-5} K^{-1}. The little structural differences indicated that the hydration sites were invariant between the two temperatures.

Fig. 1 illustrates the distribution of the identified hydration water molecules around a hetero-tetramer occupying a crystallographic asymmetric unit. The hydration water molecules distribute densely on the surface of the tetramer and form small aggregates through forming networks of hydrogen bonds as well as in the cryogenic crystal structures of other proteins [12,15]. In addition, the molecules distribute mainly on flat surface and in surface grooves, and the distribution seems to be out of correlation with the surface electrostatic potential of the tetramer (Fig. 1b).

The amount of identified hydration water molecules at 112 K was twice of that at ambient temperature (Table 1) [22], despite the fact that the resolution of the present analysis was lower than that at ambient temperature [22]. This result indicates a great potential of the cryogenic method

to investigate the hydration structures of proteins. In particular, the amount of molecules in the 'contact' class increased to six times of that at ambient temperature (Table 1) and was advantageous to discuss the roles of hydration water molecules in the molecular association. Identified 11 sulfate ions contributed little to the molecular packing. In the following sections, we focus on the hydration structures in the 'first-layer' class assisting the tetramer formation and those in the 'contact' class.

3.1. Hydration structures contributing to the association of hetero-dimers

In a crystallographic asymmetric unit, the toxin forms the $\alpha_2\beta_2$ hetero-tetramer in a head to tail association mode (Fig. 1) through facing the highly hydrophobic α-helices (α1) and the β-strands (β2) of the α subunits. The interaction between the subunits is very weak [no hydrogen bonds ($<$ 3.4 Å) and 1 van der Waals contact ($<$3.7 Å)].

Two α1-helices are distant 7-8 Å from each other, and a hydration layer composed of 25 water molecules fills the highly hydrophobic groove between the helices. Several polygonal arrangements of hydration water molecules (water molecules 1-2-3-4, 3-4-5-7-6, 6-7-9-10-8 and so on in Fig. 2a) cover the hydrophobic surface and extend the networks of hydrogen bonds along the groove. The carbonyl oxygen atoms of Ala60 and Gln63, slightly deviating from the ideal geometry in the helices, provide hydrogen-bond arms toward the groove.

On another interface of the tetramer (Fig. 2b), one planar hydration layer composed of 23 water molecules intercalates between the β2-strands. In this region, the two strands are too apart (more than 6 Å) to form an anti-parallel β-sheet, and only Trp152s interact via van der Walls contacts. The hydration water molecules just located at the positions suitable for mediating the hydrogen bonds between main chain polar atoms from the strands.

3.2. Hydration water molecules contributing to the association of the hetero-tetramers in the crystalline state

The water molecules mediating the crystal contacts were identified unambiguously from the electron density maps as shown in Fig. 2c. In an crystallographic asymmetric unit, one tetramer contacts mainly with 5 symmetry related ones (Mol 1-5 in Fig. 1a). Because two contact modes are crystallographically equivalent with the other, we focus on the three types of association modes illustrated in Fig. 3.

The parameters characterizing the crystal contacts are summarized in Table 2. The amount of water molecules assisting the contacts varies depending on the area used in the contacts, and one or two layers of the molecules intercalate into the interface (see Fig. 2c). As a result, the number of hydrogen bonds assisted by hydration water molecules is approximately 10 times larger than that formed by the tetramers alone (Table 2). The hydration water molecules surround the contact area so as to assist the weak interactions between proteins and to make the surface shape complementary (Fig. 3a,c). Of the contact modes, that with Mol 3 is weak in comparison with the other two with respect to the surface area used in the contacts and the number of possible interactions formed (Fig. 3b and Table 2).

Fig. 1. (a) Distribution of hydration water molecules around the hetero-tetramer of the killer toxin occupying a crystallographic asymmetric unit. The tetramer is illustrated as a diagram of secondary structures specified by the DSSP program [35]. The structural model of the α-subunits are colored in orange and those of β-subunits are in yellow. The names of the secondary structures are presented. The colored spheres represent the hydration water molecules identified. The green-colored spheres indicate the positions of the hydration water molecules in the 'first-layer' class (see Section 2), and those in red are in the 'second-layer' class. The hydration water molecules engaged in crystal contacts with Mol 1 and 2 are colored in cyan, those with Mol 3 in blue, and with Mol 4 and 5 in yellow. (b) The distribution of hydration water molecules on the surface of the hetero-tetramer. The molecular surface of the toxin is presented with the surface potential. The spheres are hydration water molecules and are colored in the same way with panel (a). Some names of secondary structures are indicated on the molecular surface. The yellow dashed line indicates the large hydrophobic groove between the two hetero-dimers (see also Fig. 2a). This panel is produce with using GRASP [36].

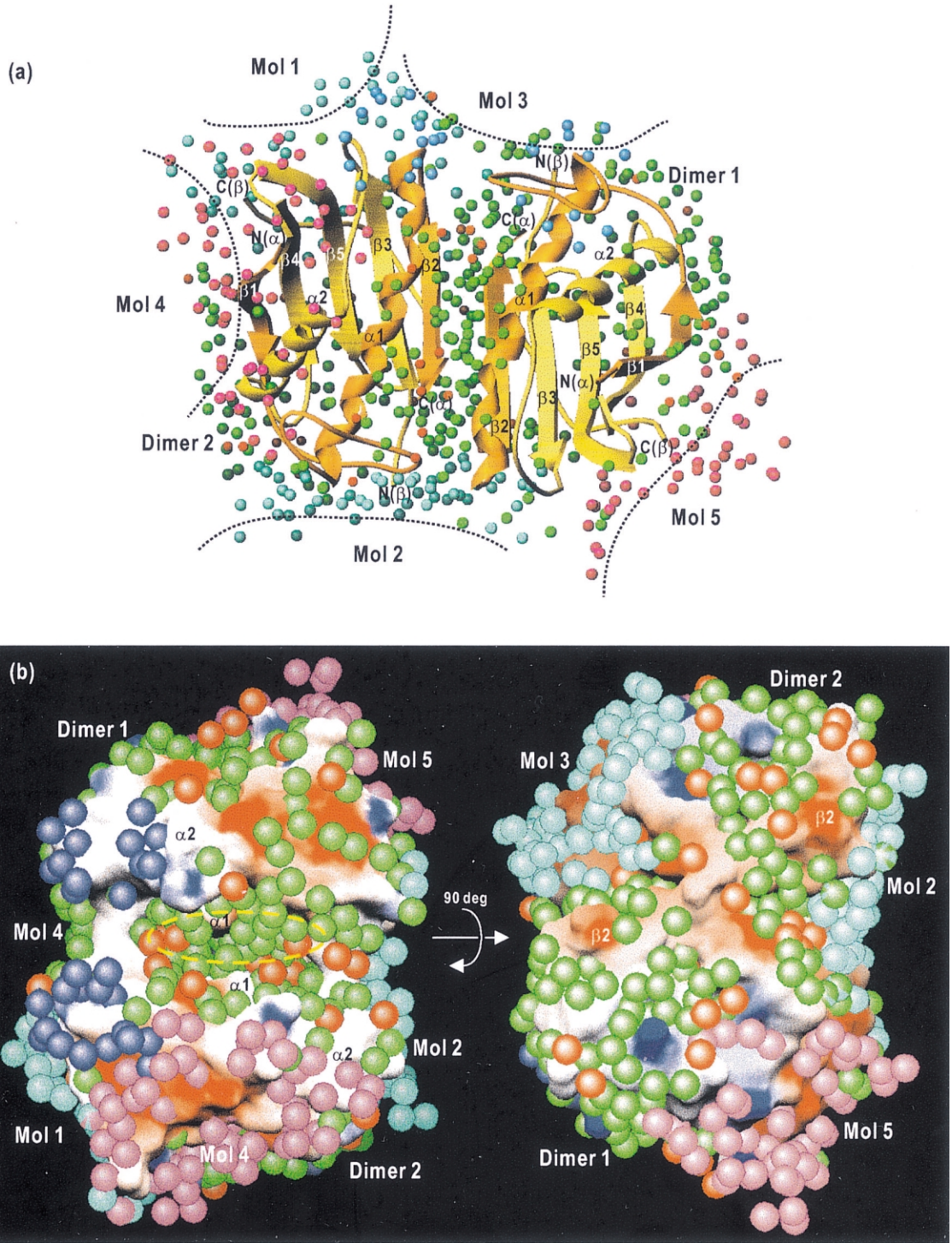
(a)
Mol 1
Mol 3
Dimer 1
Mol 4
Dimer 2
Mol 2
Mol 5
C(β)
N(α)
β4
β5
β3
β2
β1
α2
α1
C(α)
N(β)
(b)
Dimer 1
Mol 5
α2
Mol 4
α1
Mol 2
Mol 1
Dimer 2
90 deg
Dimer 2
Mol 3
β2
Mol 2
Mol 5
Dimer 1

Fig. 1.

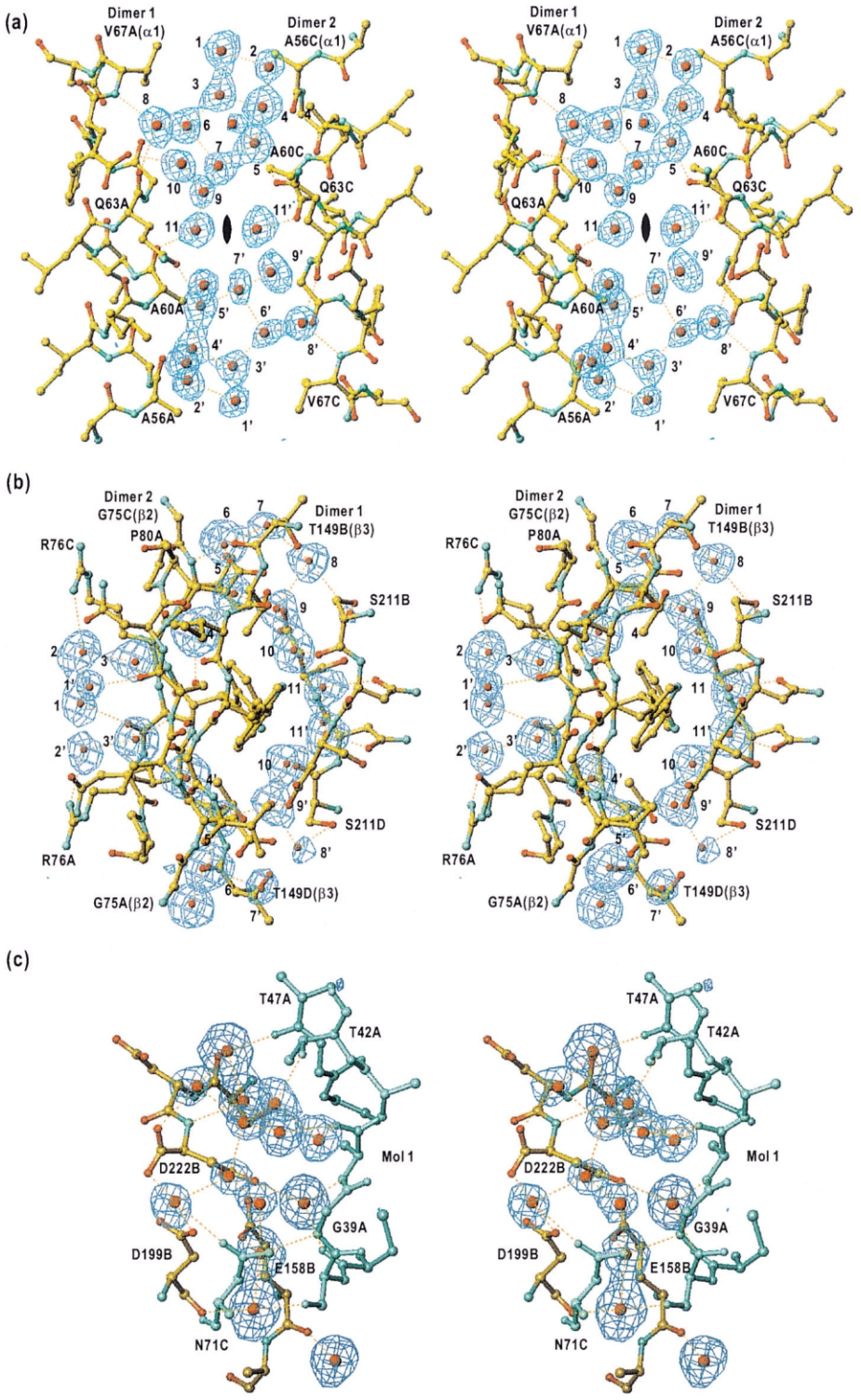
(a)
Dimer 1
V67A(α1)
Dimer 2
A56C(α1)
A60C
Q63C
Q63A
A60A
A56A
V67C
(b)
Dimer 2
G75C(β2)
P80A
Dimer 1
T149B(β3)
R76C
S211B
S211D
R76A
G75A(β2)
T149D(β3)
(c)
T47A
T42A
Mol 1
D222B
G39A
D199B
E158B
N71C

Fig. 2.

Table 1
Statistics in the collected diffraction data and the refined structural models

Diffraction data collection	
Space group	$P4_32_12$
Lattice constants (Å)	$a=79.60$, $b=79.60$, $c=118.52$
Crystal size (mm^3)	$0.1\times0.1\times0.1$
Resolution (Å)	90.0–2.1
Number of reflections	309 917
Unique reflections	22 958
Redundancy[a]	13.5
Completeness (%) (last shell)[b]	99.9 (100.0)
$I/\sigma(I)$ (last shell)[b]	35.5 (8.4)
R^I_{merge} ($I>1\sigma(I)$)[c]	0.081
Structure refinement	
Resolution (Å)	8.0–2.1
Reflections used ($F>2\sigma$ (F))	21 850
R-factor[d]	0.151
R_free[e]	0.215
Number of non-H protein atoms	1988
Number of sulfate ions in the model	11
Number of hydration water molecules	451 (224)[f]
Inside class	4 (4)[f]
First layer class	289 (171)[f]
Second layer class	56 (32)[f]
Contact layer class	102 (17)[f]
r.m.s. deviation from ideal case[g]	
Bond (Å)	0.012
Angle (°)	2.232
r.m.s. difference in main-chain atoms between two heterodimers (Å)	0.35
Solvent accessible surface ($Å^2$)[h]	
Hetero-dimer 1 free/in hetero-tetramer	5772.5/5173.8
Hetero-dimer 2 free/in hetero-tetramer	5751.7/5157.3

[a] Number of observations/unique reflections.

[b] Last shell 2.15 to 2.10 Å.

[c] $R^I_{merge}=\sum_h\sum_i\left|I_i(h)-\langle I(h)\rangle\right|/\sum_h\sum_i I_i(h)$, where $I_i(h)$ is the intensity of the i-th observation of reflection h.

[d] $R=\sum_h\left|F_{obs}(h)-F_{calc}(h)\right|/\sum_h F_{obs}(h)$, where $F_{obs}(h)$ and $F_{calc}(h)$ are the observed and calculated structure factors of reflection h, respectively.

[e] The *R_free* factor was calculated for the 10% of unique reflections, which were not used in the structure refinement throughout [34].

[f] The number of hydration water molecules obtained by analyzing the coordinate at ambient temperature [20].

[g] Root-mean-square (r.m.s.) deviations from ideal stereochemical geometry.

[h] The surface area were calculated by the Connolly's method [27].

Fig. 2. Stereo-plots showing the arrangement of hydration water molecules located at the interface of hetero-tetramers and crystal contact area. Ball-and-stick models show the polypeptide chains, and the small red spheres indicate the positions of hydration water molecules. The blue fishnets are omit-annealed difference electron density map calculated using the reflections between the Bragg spacings of 8.0–2.1 Å and contoured at 3.5 standard deviation level from the average of the map. Several hydration water molecules are numbered for clarity, and the names of some residues are inserted. The orange dashed lines present the possible hydrogen bonds between hydration water molecules and polar atoms of proteins. (a) The distribution of hydration water molecules in the large groove formed between two α1 helices. The symbol at the center indicates the position of pseudo-diad axis relating the two hetero-dimers. The distribution of hydration water molecules between β2 strands (b) and at the contact area with Mol 1 (c).

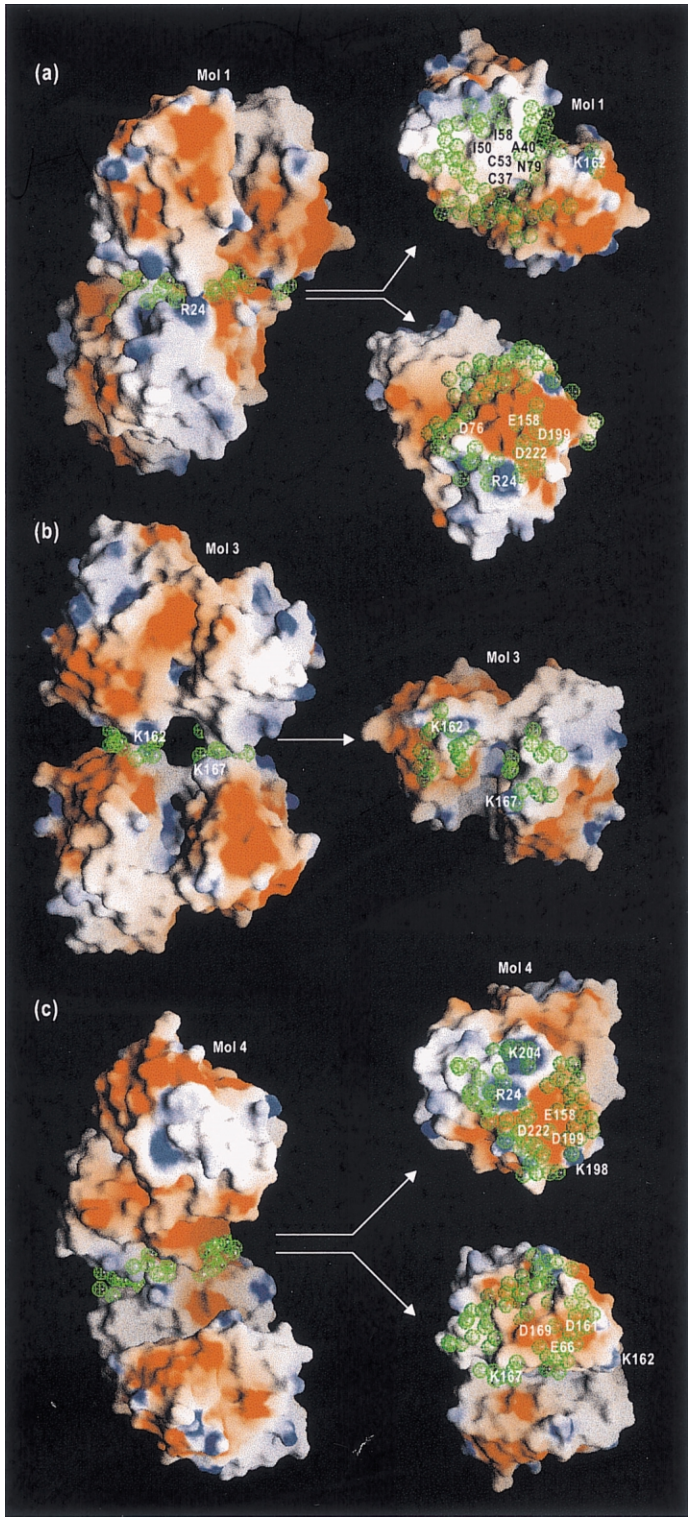
(a)
Mol 1
R24
Mol 1
I58
I50
A40
C53
N79
K162
C37
D76
E158
D199
D222
R24
(b)
Mol 3
K162
K167
Mol 3
K162
K167
(c)
Mol 4
Mol 4
K204
R24
E158
D222
D199
K198
D169
D161
E66
K162
K167

Fig. 3.

Table 2
The characteristic parameters in the contact area

Interface	Area used (Å)[a]		Number of	Number of protein–protein interactions[c]		Number of
	protein–protein	include water	water molecules[b]	H-bonds	van der Waals contacts	possible H-bonds with water molecules
Mol 1	590.6	1126.7	60	5	15	84
Mol 3	265.6	582.0	28	0	3	17
Mol 4	476.0	1015.2	59	9	16	70

[a] The surface areas were calculated by Connolly's method [27].
[b] The figures include the hydration water molecules hydrating the adjoining molecules related by crystallographic symmetry operations.
[c] The number of possible interactions are counted for hydrogen bonds within 3.4 Å and for possible van der Waals contacts within 3.7 Å.

The electrostatic property of the contacting surface is one of important factors to ensure the stable association of the toxin molecules. For instance, at the interface between the tetramer and Mol 1 (Fig. 3a), the negatively charged surface of the tetramer faces to the hydrophobic and neutral surface of Mol 1. Because the tetramer is crystallized under an acidic pH condition [18], the negative charge on Mol 1 is presumably neutralized. In contrast, in the contact with Mol 4 (Fig. 3c), the surface potentials are complementary between the contacting tetramers, because Arg24 and Lys204 are located on the surface of Mol 4 in facing the negatively charged surface of the tetramer. Therefore, this contact mode may be more advantageous than that with Mol 1 to shield the negatively charged surface from bulk solvent.

Even at the crystal contact area, the water molecules retain the standard tetrahedral interaction geometry (Fig. 4), indicating that the molecular contacts occur to satisfy the standard geometry. In addition, the average number of interactions per one hydration water molecule in the 'contact' class is 3.6, significantly larger than that in the first layer class (3.0). This difference is common in various cryogenic crystal structure analyses [12,15], reflecting the possibility that the 'contact' class hydration water molecules are artificially formed in the association. However, the difference must be important to ensure the stable intermolecular interactions at the crystal contact area.

The standard tetrahedral interaction geometry enables the three-dimensional extension of the hydrogen-bond networks at the contact area (Fig. 5). At the interface with Mol 1, a network covers the highly acidic region composed of Glu158, Asp199 and Asp222 (Fig. 3a) and extends to the edge of two α1-helices in Mol 1 (cyan-colored water molecules in Fig. 5a). In the opposite face of the contact area, a large network shields the hydrophobic surface around the α1-β2 loop from bulk solvent (green-colored water molecules in Fig. 5a). In the contact with Mol 3, where a few van der Waals contacts are formed between two tetramers (Table 2), the networks covering Lys162 contribute significantly the association at the tips of the tetramers (Fig. 5b). Between the tetramer and Mol 4 (Fig. 5c), three networks surround the contact area so as to isolate Glu158, Asp199 and Asp222 from bulk solvent. The networks also connect indirectly the three acidic residues and Arg24, Lys198 and Lys204 located at the contact region.

Fig. 3. Illustrations showing the crystal contact modes with Mol 1 (panel a), Mol 3 (b) and Mol 4 (c). The molecular surface is presented with the electrostatic potential and the hydration water molecules are shown with green-colored fishnets. Names of residues engaged in crystal contacts are superimposed on the surface. This figure is drawn with the program GRASP [36].

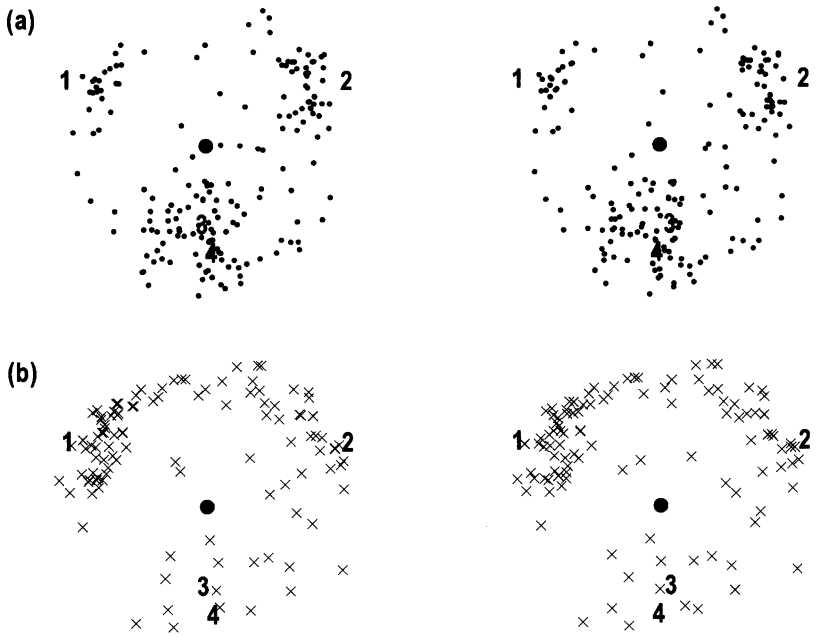

Fig. 4. Stereo-plots showing the geometry of hydrogen bonds (a) between hydration water molecules and (b) between hydration water molecules and polar atoms of proteins. Hydration water molecules having more than three hydrogen bonds partners are chosen from the 'contact' class, and their geometry in hydrogen bonds is compared with the standard geometry of hydrogen bonds in a water molecule through a least square calculation. This figure is produced with the program FESTKOP [12,15]. The numbers 1–4 indicate the positions of donor and/or acceptor atoms in the ideal hydrogen bond geometry.

As a result, crystal contact modes at the interfaces with Mol 1 and Mol 4 have great contribution to the crystal packing. The substantial difference between the two modes is the complementarity in the electrostatic potentials of the surface used in the contacts (Fig. 3a,c).

4. Discussion

In the present study, we analyzed the characteristics of hydration structures assisting the association of the killer toxin molecules in a crystalline state. Here, we discuss the possibility that any of the association modes observed in the crystalline state prevents the irreversible dissociation of the hetero dimer in the physiological pH condition. In addition, we also discuss the molecular association from the point of view of physicochemical theory on solvent in confined geometry.

4.1. Implications of the association modes of the killer toxin molecules in their biological function

Under the physiological pH conditions in vitro, the αβ hetero-dimer dissociates irreversibly into

Fig. 5. Networks of hydrogen bonds at the contact areas with Mol 1 (a), Mol 3 (b) and Mol 4 (c). The secondary structures of the toxin molecules are shown in the same scheme in Fig. 1a. The large spheres indicate the positions of hydration water molecules residing around the crystal contact area and are colored to distinguish the networks. Sticks show possible hydrogen bonds at the contact area, and the small ball-and-stick models are the residues engaged in the networks. Names of some residues are indicated. (a) Two large networks at the contact site with Mol 1. A network is composed of 18 hydration water molecules (cyan colored spheres) and 25 polar protein atoms, and another 33 water molecules (green colored) and 24 protein atoms. (b) Four small networks at the contact area with Mol 3. (c) Two large networks at the contact site with Mol 4: one composed of 25 water molecules (colored in cyan) and 25 protein atoms, and another 10 water molecules (colored in purple) and 18 protein atoms. The spheres colored in green are 7 water molecules composing an additional small network. This Figure is produced with the programs FESTKOP [12,15] and MOLSCRIPT [37].

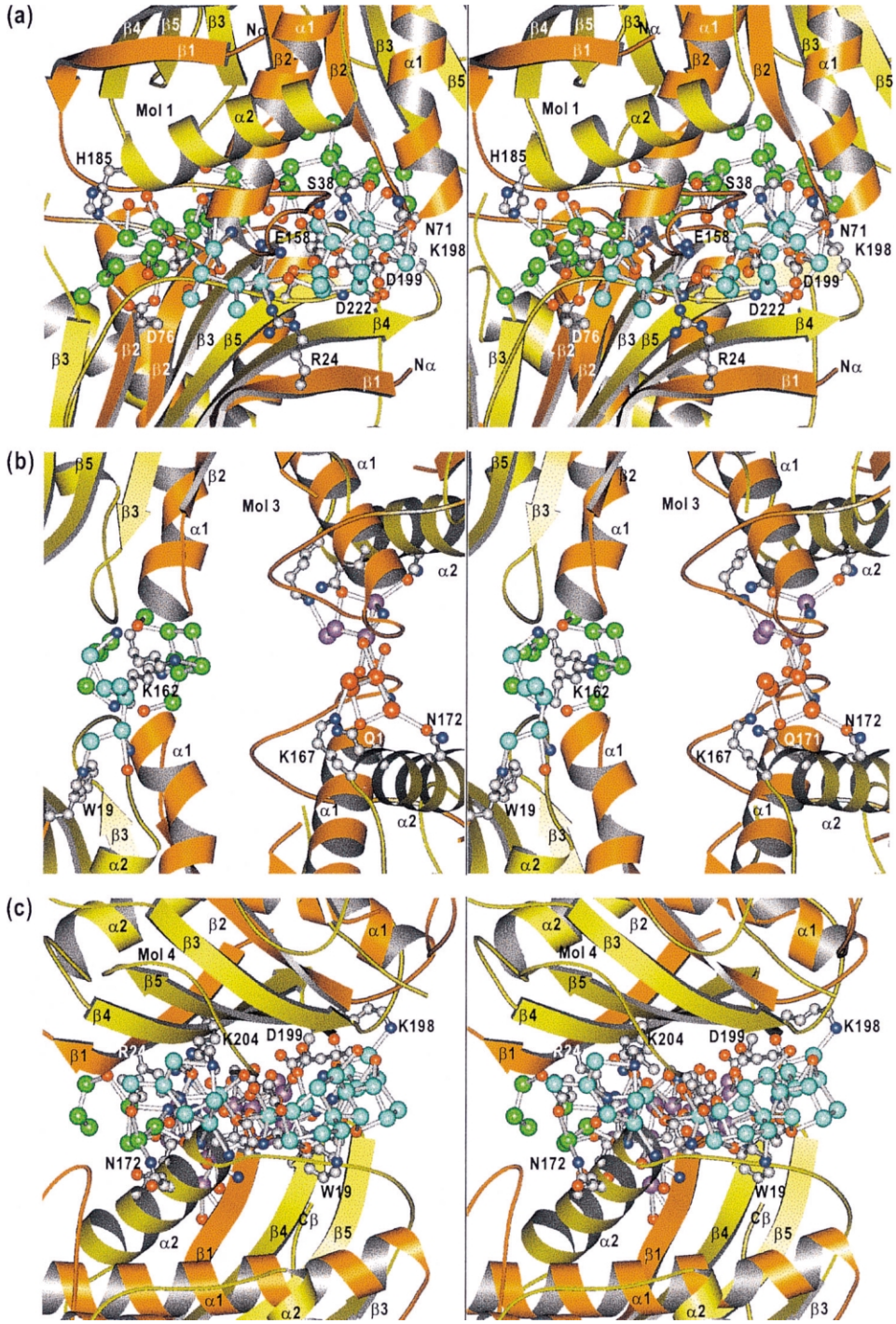
(a)
Mol 1
H185
S38
E158
N71
K198
D199
D222
D76
R24
Nα
(b)
Mol 3
K162
K167
N172
Q171
W19
(c)
Mol 4
K204
D199
K198
R24
N172
W19
Cβ

Fig. 5.

the two polypeptide chains [19–21]. However, it is believed that the toxin works as dimer under the neutral pH conditions in cells. One possibility to explain the killer activity is the formation of higher order structures preventing the dissociation. Here, we examine the possibility that any intermolecular interaction mode in the crystal may be suitable to prevent the dissociation of αβ-dimer.

At the dimer–dimer interface, the hydration water molecules assist the interactions through a number of hydrogen bonds. Although this finding suggests the indispensable roles of the hydration water molecules in the association of the dimers, the association mode is not advantageous to prevent the dissociation of subunits by the following reasons. In comparison with the hydration-mediated formation of the quaternary structures observed in an Fv fragment of immunoglobulin G [13] and nitrile hydratase (NHase) [31], the direct protein–protein interactions are too little. In fact, the αβ-dimer rather than the $\alpha_2\beta_2$-tetramer is a major component in solution [19]. In addition, the electrostatic repulsion between Glue158, Asp119 and Asp222 is believed to initiate the dissociation of the subunits [22]. The highly acidic surface is still exposed to bulk solvent in this contact mode.

Therefore, any association mode shielding the highly acidic area from bulk solvent is suitable to prevent the irreversible dissociation of the dimer. In this regard, those with Mol 1 and Mol 4 are suitable to shield the area among the contact modes found (Figs. 3 and 5). With respect to the total number of interactions formed, the crystal contact with Mol 1 is the most stable (Table 2, Figs. 3 and 5). However, it may be unlike in solution at medium pH range, because of the electrostatic properties of the contacting area as described in the Section 3.

In contrast, the contact with Mol 4 seems to be suitable with respect to the electrostatic interaction. In addition, the number of hydrogen bonds formed between the dimers is nearly twice of that in the contact with Mol 1 (Table 2), and the networks of hydration water molecules shield the negatively charged cluster (Fig. 5). A slight reorientation of the two dimers seems to be more favorable to make the electrostatic properties of contacting surface more complementary (Fig. 3). Therefore, this contact mode is the most energetically stable among the association modes in the crystal and may be a candidate for ensuring the association of the dimers even in the physiological aqueous environment.

In this contact mode, hydration water molecules intercalate between the three acidic and three basic residues. When water molecules are set in an electrostatic field, the molecules are orientationally ordered [32]. The ordering results a small Kirkwood *g*-factor [33]. Therefore, the hydration water molecules connecting the charged residues are probably orientational ordering and bridging the electrostatic interactions between the residue as observed in molecular dynamics simulations on water molecules sandwiched between charged amino acid residues [32] and in the active-site cleft of human lysozyme (Higo and Nakasako, submitted).

Of course, ions or small biological molecules in cells may have influences on the association of two polypeptide chains. In fact, sodium chloride or potassium chloride enhances the killer activity of the toxin [17]. When monovalent ions attaching on the contact area with Mol 4, they may work to suppress the electrostatic repulsion in the cluster of acidic residues under the physiological pH conditions.

4.2. Comparison of the distribution of water molecules in crystal contact area with the theoretical prediction on the solvent molecules in confined geometry

Fig. 6a shows the histogram of the distance between the protein atoms located at the crystal contact area (see Fig. 1). The plot has two maxima near 4.0 Å and 6.5 Å, implying that the protein atoms distribute regularly rather than randomly. When the atom radius is taken into consideration, the surface of pairs of tetramers in contact separates 2.6 and 4.0 Å. The individual peak in the histogram corresponds likely to the separation of surface sandwiching one or two layers of the hydration water molecules.

Theoretical studies on solvent molecules in confined geometry have predicted an oscillatory sol-

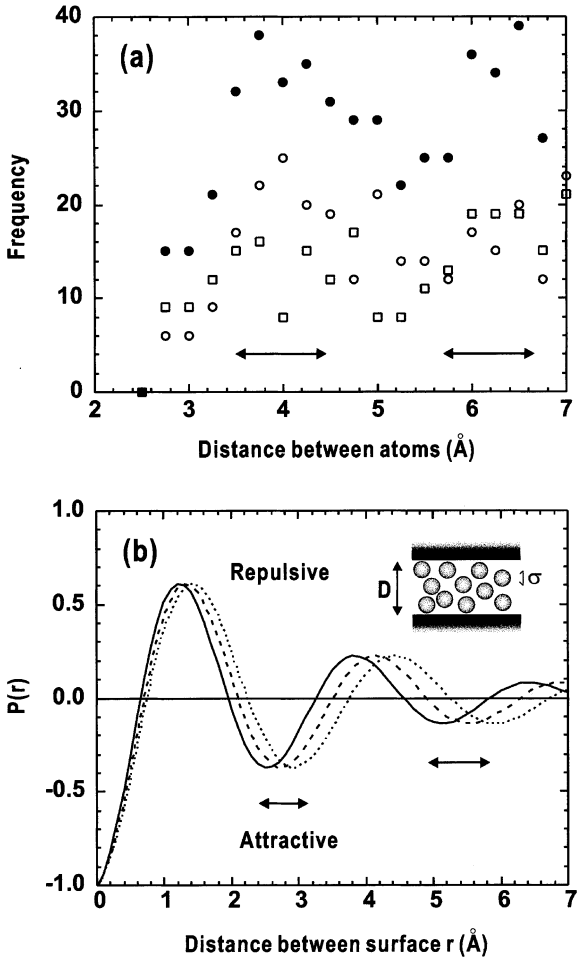

Fig. 6. (a) A histogram of the distance between the atom pairs in the crystal contacts. The distance presented here is that from a target atom in a tetramer to the closest atom in the neighboring tetramer. The histogram of the distance are summed and plotted as to the crystal contacts with 1 and 2 (symbol ○) and those with 4 and 5 (symbol □) and their total (symbol ●). (b) The solvation pressure as given by Eq. (1) for solvent particle radius of 2.5 (dashed line), 2.8 (dotted line) and 3.0 Å (solid line). The arrows indicate the area, within which attractive interaction between the two solid surfaces is expected.

vation force between solid surface separated within several molecular diameters of solvent molecules [16,23,24]. As a first approximation, the pressure between two flat surface sandwiching solvent molecules with a diameter of σ (inset in Fig. 6b) is described by an exponentially decaying cosine function:

$$P(D) \approx -k_B T \rho_s \cos(2\pi D/\sigma)\exp(-D/\sigma) \quad (1)$$

where D is the distance between two flat surface (see inset of Fig. 6b), and ρ_s is approximately equal to the density of bulk solvent. In Fig. 6b, $P(D)$ values are calculated in the cases of $\sigma = 2.5$, 2.8 and 3.0 Å. Between the flat surface, attractive forces are significant at a period of the diameter of solvent molecule [24]. The calculated $P(D)$ for $\sigma = 2.5 \sim 2.8$ Å likely explains both the observed optimum distances between the molecular surface of killer toxin in crystal contacts (Fig. 6a).

This correlation between the experiment and the theory suggests that the theory on solvation force may be applicable in studying the molecular association of proteins in crystals and molecular recognition. It is very interest to examine further the correlation between the theoretical and experimental results for more than 15 000 crystal structures in the PDB. The utilization of the huge number of structural data may help to refine the theory on water molecules in confined geometry.

Because many biological macromolecules form various types of molecular complexes via Mie potential, the investigations on the association modes of macromolecules in crystals including the hydration water molecules may help to predict the surface used in molecular recognition in the future.

Acknowledgments

The authors express their gratitude for Dr C. Suzuki (National Food Institute, Ministry of Agriculture, Forestry and Fisheries) for her help in the sample preparation. This work was supported partly by the grants-in-aid from the Ministry of Education, Science, Sports and Culture of Japan to M. N.

References

[1] A. Ducruix, R. Giegé, Crystallization of Nucleic Acids and Proteins. A Practical Approach, IRL Press, Oxford, 1992.
[2] A. McPherson, Preparation and Analysis of Protein Crystals, Wiley, New York, 1982.

[3] M Riés-Kautt, A. Ducruix, in: C.W. Carter, R.M. Sweet (Eds.), Macromolecular Crystallography, Methods in Enzymology, 276, Academic Press, London, 1997, pp. 23–59.
[4] E.J.W. Verwey, J.T.G. Overbeek, Theory of the Stability of Lyophobic Colloids, Elsevier, Amsterdam, 1948.
[5] T.N. Bhat, G.A. Bentley, G. Boulot, et al., Bound water molecules and conformational stabilization help mediate an antigen-antibody association, Proc. Natl. Acad. Sci. USA 91 (1991) 1089–1093.
[6] D.G. Covell, A. Wallqvist, Analysis of protein–protein interactions and the effects of amino acid mutations on their energetics. The importance of water molecules in the binding epitope, J. Mol. Biol. 269 (1997) 281–297.
[7] A.M. Bonvin, M. Sunnerhagen, G. Otting, W.F. van Gunsteren, Water molecules in DNA recognition II: a molecular dynamics view of the structure and hydration of the trp operator, J. Mol. Biol. 282 (1998) 859–873.
[8] L.A. Labeots, M.A. Weiss, Electrostatics and hydration at the homeodomain–DNA interface: chemical properties of an interfacial water cavity, J. Mol. Biol. 269 (1997) 113–128.
[9] D.C. Mitchell, B.J. Litman, Effect of protein hydration on receptor conformation: decreased levels of bound water promote metarhodopsin II formation, Biochemistry 38 (1999) 7617–7623.
[10] E.N. Baker, T.L. Blundell, J.F. Cutfield, et al., The structure of 2Zn pig insulin crystals at 1.5 Å resolution, Phil. Trans. R. Soc. London B Biol. Sci. 318 (1988) 369–456.
[11] E.F. Garman, T.R. Schneider, Macromolecular cryocrystallography, J. Appl. Cryst. 30 (1997) 211–237.
[12] M. Nakasako, Large-scale networks of hydration water molecules around β-trypsin revealed by cryogenic X-ray crystal structure analyses, J. Mol. Biol. 289 (1999) 547–564.
[13] M. Nakasako, H. Takahashi, N. Shimba, I Shimada, Y. Arata, The pH-dependent structural variation of complementary-determining region H3 in the Fv fragment from an anti-dansyl monoclonal antibody, J. Mol. Biol. 291 (1999) 177–184.
[14] M. Nakasako, T. Fujisawa, S. Adachi, T. Kudo, S. Higuchi, Large-scale domain movements and hydration structure changes in the active site cleft of unligated glutamate dehydrogenase from *Thermococcus profundus* by cryogenic X-ray crystal structure analysis and small-angle X-ray scattering, Biochemistry 40 (2001) 3069–3079.
[15] M. Nakasako, Large-scale networks of hydration water molecules around proteins investigated by cryogenic X-ray crystallography', Mol. Cell. Biol. 47 (2001) 767–790.
[16] J. Israelachivili, Intermolecular and Surface Forces, Academic Press, London, 1985.
[17] C. Suzuki, S. Nikkuni, The primary and subunit structure of a novel type killer toxin produced by a halotolerant yeast, *Pichia farinosa*, J. Biol. Chem. 269 (1994) 3041–3046.
[18] N. Kunishima, T. Kashiwagi, C. Suzuki, et al., Crystallization and preliminary X-ray diffraction studies of a novel killer toxin from a halotolerant yeast *Pichia farinosa*, Acta Crystallogr. Sect. D 53 (1997) 112–113.
[19] S.W. Price, F. Tsuchiya, C Suzuki, Y. Arata, Characterization of the solution properties of *Pichia farinosa* killer toxin using PGSE NMR diffusion measurements, J. Biomol. NMR 13 (1999) 113–117.
[20] C. Suzuki, T. Kashiwagi, F. Tsuchiya, et al., Circular dichroism analysis of the interaction between the alpha and beta subunits in a killer toxin produced by a halotolerant yeast, *Pichia farinosa*, Protein Eng. 10 (1997) 99–101.
[21] T. Kashiwagi, N. Yamada, K. Hirayama, et al., An electrospray-ionization mass spectrometry analysis of the pH-dependent dissociation and denaturation processes of a heterodimeric protein, J. Am. Soc. Mass Spect. 11 (2000) 54–61.
[22] T. Kashiwagi, N. Kunishima, C. Suzuki, et al., The novel acidophilic structure of the killer toxin from halotolerant yeast demonstrates remarkable folding similarity with a fungal killer toxin, Structure 5 (1997) 81–94.
[23] W. van Megen, I.K. Snook, Solvent structure and solvation forces between solid bodies, J. Chem. Soc. Faraday II 75 (1970) 1095–1102.
[24] P. Tarazona, L. Vicente, A model for density oscillation in liquids between solid walls, Mol. Phys. 56 (1985) 557–572.
[25] Z. Otwinowski, W. Minor, in: C.W. Carter, R.M. Sweet (Eds.), Macromolecular Crystallography, Methods in Enzymology, 276, Academic Press, London, 1997, pp. 307–326.
[26] F.C. Bernstein, T.F. Koetzle, G.J.B. Williams, et al., The Protein Data Bank: A computer based archival file for macromolecular structure, J. Mol. Biol. 112 (1978) 535–542.
[27] A.T. Brünger, X-PLOR Version 3.1. A System for X-ray Crystallography and NMR, Yale University Press, New Haven, CT, 1993.
[28] R.A. Engh, R. Huber, Accurate bond and angle parameters for X-ray protein structure refinement, Acta Crystallogr. Sect. A 47 (1991) 392–400.
[29] M.L. Connolly, Solvent-accessible surfaces of proteins and nucleic acids, Science 221 (1983) 709–713.
[30] H. Frauenfelder, H. Hartmann, M. Karplus, et al., Thermal expansion of a protein, Biochemistry 20 (1987) 254–261.
[31] M. Nakasako, M. Odaka, M. Yohda, et al., Tertiary and quaternary structures of photoreactive Fe-type nitrile hydratase from *Rhodococcus* sp. N-771: roles of hydration water molecules in stabilizing the structures and the structural origin for the substrate specificity of the enzyme, Biochemistry 38 (1999) 9887–9898.

[32] J. Higo, M. Sasai, H. Shirai, H. Nakamura, T. Kugimiya, Large vortex-like structure of dipole field in computer models of liquid water and dipole-bridge between biomolecules, Proc. Natl. Acad. Sci. USA 98 (2001) 5961–5964.

[33] J.G. Kirkwood, Statistical mechanics of fluid mixtures, J. Chem. Phys. 3 (1935) 300–313.

[34] A.T. Brünger, Free R value: a novel statistical quantity for assessing the accuracy of crystal structures, Nature 355 (1992) 472–475.

[35] W. Kabsch, C. Sander, Dictionary of protein secondary structure: pattern recognition of hydrogen bonded and geometrical features, Biopolymers 22 (1983) 2577–2637.

[36] A. Nicholls, K.A. Sharp, B. Honig, Protein folding and association; insights from the interfacial and thermodynamic properties of hydrocarbons, Proteins Struct. Funct. Genet. 11 (1991) 281–296.

[37] P.J. Kraulis, MOLSCRIPT: a program to produce both detailed and schematic plots of protein structures, J. Appl. Cryst. 24 (1991) 946–950.